East European Journal of Physics. 2. 191-202 (2026)
DOI:10.26565/2312-4334-2026-2-20 ISSN 2312-4334

EXPERIMENTAL AND SIMULATION-BASED STUDY ON THE STRUCTURAL, OPTICAL, AND MECHANICAL PROPERTIES OF PLA/ZnO NANOCOMPOSITES

Fakhriddin T. Yusupov[1]*, Tokhirbek I. Rakhmonov[1], Mekhriddin F. Akhmadjonov[1], Dilobarbonu E. Abdukodirova[2], Yelmurat Dosymov[3], Iftikhorjon I. Yulchiev[1]
[1]*Fergana State Technical University, Fergana, Uzbekistan*
[2]*Chirchik State Pedagogical University, Chirchik, Uzbekistan*
[3]*Khoja Akhmet Yassawi International Kazakh-Turkish University, Kazakhstan*
**Corresponding Author e-mail: yusupov.fizika@gmail.com*
Received January 13, 2026; revised April 27, 2026; accepted May 2, 2026

This work presents a comprehensive experimental and theoretical investigation of polylactide (PLA) nanocomposites reinforced with zinc oxide (ZnO) nanoparticles at concentrations of 0.5, 1, 3, and 5 wt.%. The dispersion state and microstructural features of ZnO within the PLA matrix were examined using scanning electron microscopy combined with energy-dispersive X-ray spectroscopy, revealing homogeneous distribution at low filler contents and progressive agglomeration at higher loadings. X-ray diffraction analysis confirms that ZnO preserves its hexagonal wurtzite crystal structure after incorporation into the polymer matrix, while composition-dependent variations in crystallite size and lattice microstrain are found to correlate with the mechanical response of the composites. Fourier-transform infrared spectroscopy indicates interfacial interactions between PLA chains and ZnO nanoparticles, as evidenced by systematic shifts in the carbonyl stretching band and associated charge redistribution. Ultraviolet–visible spectroscopy demonstrates a significant enhancement of UV-shielding performance with increasing ZnO content, accompanied by the emergence of sub-bandgap absorption tails attributed to defect-related and interfacial electronic states. Density functional theory calculations support the experimental observations by revealing interfacial charge transfer and a slight modification of the electronic structure at the PLA/ZnO interface. The results show that ZnO incorporation improves both mechanical stiffness and UV-blocking efficiency, while an optimal ZnO loading below 1 wt.% is identified to maintain mechanical integrity and minimize agglomeration-induced degradation.
Keywords: *PLA/ZnO nanocomposites; UV-shielding; Mechanical properties; XRD; FTIR; DFT simulations; Charge transfer; Nanomaterials; Polymer reinforcement*
PACS: 78.20.-e, 73.61.Ga, 85.60.-q, 68.55.-a

1. INTRODUCTION

Polylactide (PLA) has emerged as one of the most promising biodegradable polymers due to its renewable origin, biocompatibility, and suitability for packaging, biomedical devices, and environmentally sustainable applications [1]. Despite these advantages, neat PLA generally exhibits limited mechanical strength and poor resistance to ultraviolet (UV) radiation, which significantly restricts its long-term stability and performance under practical service conditions [2]. As a result, considerable research efforts have been devoted to improving the functional properties of PLA by incorporating inorganic fillers and nanostructured reinforcements. Among various inorganic additives, zinc oxide (ZnO) has attracted particular attention owing to its wide direct bandgap (~3.3 eV), strong UV absorption capability, chemical stability, and biocompatibility. In addition, ZnO exhibits multifunctional physical properties, including semiconductivity, piezoelectricity, and surface polarity, which make it a suitable candidate for enhancing both mechanical and optical characteristics of polymer-based nanocomposites [3,4]. Previous studies have demonstrated that ZnO incorporation can effectively improve UV-shielding efficiency and stiffness in PLA-based systems; however, these enhancements are often accompanied by challenges related to nanoparticle dispersion and interfacial compatibility [3–6]. Recent investigations on ZnO-based thin films, heterostructures, and nanocomposites have highlighted the importance of defect states, surface polarization, and charge-transfer phenomena in determining the functional properties of ZnO-containing systems [7–9]. Furthermore, theoretical studies based on density functional theory have shown that interfacial charge redistribution can modify the electronic structure and defect-related states, thereby directly affecting optical absorption and dielectric behavior in hybrid materials [10]. At higher filler concentrations, ZnO nanoparticles tend to agglomerate due to strong interparticle interactions, leading to stress concentration sites and deterioration of mechanical performance [11,12]. Therefore, achieving a uniform dispersion of ZnO and understanding the nature of interfacial interactions between the polymer matrix and the inorganic phase remain critical issues. From a fundamental perspective, the interfacial region governs stress transfer, phonon scattering, and electronic polarization effects, which collectively influence the mechanical integrity and optical response of the composite material.

Despite these advances, a systematic correlation between experimental observations and atomistic-level simulations of PLA/ZnO nanocomposites remains underexplored.

In this study, PLA/ZnO nanocomposites containing 0.5–5 wt.% ZnO are fabricated and investigated using a combined experimental and theoretical approach. The structural, mechanical, and optical properties are characterized by

Cite as: F.T. Yusupov, T.I. Rakhmonov, M.F. Akhmadjonov1, D.E. Abdukodirova, Y.Dosymov, I.I. Yulchiev, East Eur. J. Phys. 2, 191 (2026), https://doi.org/10.26565/2312-4334-2026-2-20

SEM/EDS, XRD, FTIR, and UV–Vis spectroscopy, while density functional theory calculations are employed to elucidate the electronic structure and interfacial charge transfer at the PLA/ZnO interface. By integrating experimental results with theoretical insights, this work aims to establish clear structure–property relationships and to identify an optimal ZnO loading that balances mechanical reinforcement with enhanced UV-shielding performance.

2. MATERIALS AND METHODS

Polylactide (PLA, NatureWorks 4032D) was employed as the polymer matrix, while zinc oxide (ZnO) nanopowder with an average particle size of 30–60 nm and a purity of 99.9% was used as the inorganic reinforcing phase. Prior to compounding, PLA pellets were dried under vacuum at 60 °C for 8 h to remove residual moisture, thereby preventing hydrolytic degradation and undesirable changes in melt rheology during processing, as schematically illustrated in Figure 1a. ZnO nanoparticles were incorporated into the PLA matrix at loadings of 0.5, 1, 3, and 5 wt.% to systematically evaluate the influence of filler content on the structural, optical, and mechanical properties of the resulting nanocomposites. The composites were prepared by melt blending using a laboratory-scale co-rotating twin-screw extruder (Figure 1a). The barrel temperature profile was maintained in the range of 170–185°C from the feeding zone to the die, considering the thermal stability window of PLA to avoid excessive chain scission. The screw rotation speed was set to 60 rpm, and the residence time was approximately 10 min, ensuring effective dispersion of ZnO nanoparticles in the molten polymer while minimizing thermal degradation. The extrudate strands were subsequently cooled to room temperature and pelletized (Figure 1a).

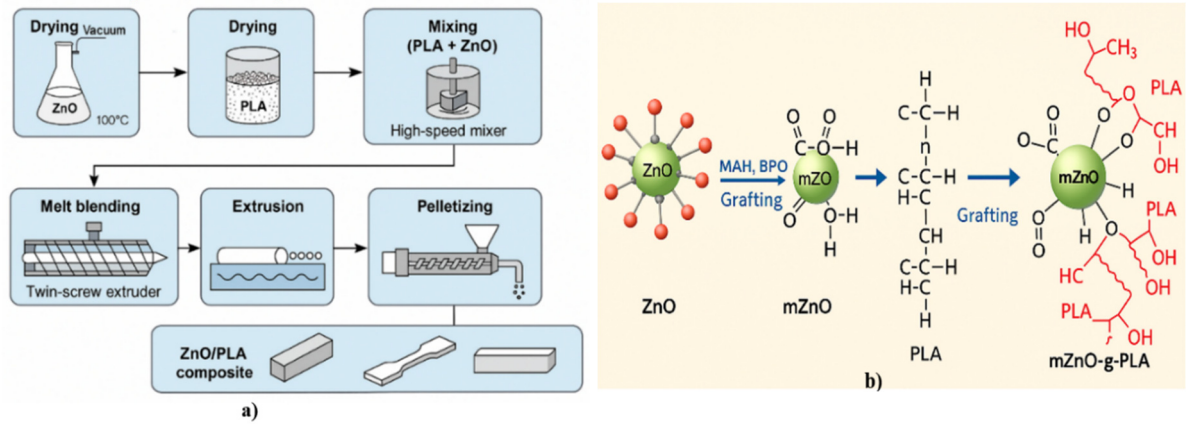

Figure 1. Preparation workflow of PLA/ZnO nanocomposites (a) and MAH/BPO-assisted surface grafting scheme (b) forming ester linkages between ZnO–COOH and PLA–OH groups

In addition, to enhance interfacial compatibility between the inorganic ZnO nanoparticles and the PLA matrix, a MAH/BPO-assisted surface grafting approach was employed. As schematically shown in Figure 1b, maleic anhydride (MAH), initiated by benzoyl peroxide (BPO), promotes the formation of ester linkages between the carboxyl groups on the ZnO surface (ZnO–COOH) and the hydroxyl end groups of PLA (PLA–OH). This chemical grafting mechanism improves interfacial adhesion, suppresses nanoparticle agglomeration, and facilitates more efficient stress transfer across the ZnO–PLA interface. Standard testing specimens were produced from the compounded pellets by injection molding. The molding temperature was maintained at 175–180 °C, and the mold clamping pressure was set to 6–7 MPa. The samples obtained were prepared for mechanical, thermal, and structural characterization in accordance with ASTM D638, ASTM D790, and ASTM D256 standards, respectively. Prior to testing, all specimens were conditioned at 23 ± 2 °C for at least 48 h to ensure reproducible equilibrium properties.

2.1 Characterization techniques

The microstructure and elemental distribution of the PLA/ZnO nanocomposites were examined by scanning electron microscopy (SEM) coupled with energy-dispersive X-ray spectroscopy (EDS). Fractured tensile specimens were used to reveal the internal morphology of the composites and to assess the dispersion state of ZnO nanoparticles within the PLA matrix. SEM provided high-resolution images of particle shape, agglomeration behavior, and fracture features, while EDS elemental mapping of Zn and O was employed to verify the spatial uniformity and stoichiometric stability of the ZnO phase inside the polymer [13,14]. The crystalline structure of the nanocomposites was analyzed by X-ray diffraction (XRD). Diffraction patterns of neat PLA and PLA/ZnO samples containing 0.5, 1, 3, and 5 wt.% ZnO were recorded to identify the characteristic reflections of the hexagonal wurtzite ZnO phase and to monitor composition-dependent changes in peak intensity, width, and position. These data were used to confirm the preservation of ZnO crystallinity after melt processing and to extract qualitative information on crystallite size and microstrain evolution within the polymer matrix. Fourier-transform infrared (FTIR) spectroscopy was used to examine the chemical structure of PLA and interfacial interactions in PLA/ZnO nanocomposites. Changes in the carbonyl (C=O) stretching and CH3 vibrational bands were analyzed to assess modifications in polymer chain packing and local amorphization induced by ZnO incorporation, while the Zn–O vibration band in the low-wavenumber region confirmed the presence of the ZnO phase. The evolution of these

bands enabled correlation between molecular-level interfacial effects and the optical and mechanical behavior of the composites [14,15].

Optical properties and UV-shielding performance were evaluated by UV–Vis spectroscopy. Absorption spectra of PLA/ZnO nanocomposites with different ZnO loadings were recorded over the near-UV–visible range and compared with those of neat PLA. The position and shape of the absorption edge, as well as the appearance of sub-bandgap tails and broad absorption features at higher filler contents, were analyzed to distinguish between intrinsic band-edge transitions of wurtzite ZnO and defect-mediated states associated with oxygen vacancies, interstitials, and interfacial defects [16]. These measurements provided direct experimental insight into how ZnO concentration and dispersion control the UV-blocking efficiency of the hybrid system.

Mechanical properties were characterized using standard tensile, flexural, and impact tests on injection-molded specimens prepared in accordance with ASTM D638, ASTM D790, and ASTM D256, respectively [10,13]. The samples were conditioned at 23 ± 2°C for at least 48 h prior to testing to ensure reproducible equilibrium behavior. The resulting stress–strain curves and impact responses were used to quantify the effect of ZnO loading on stiffness, strength, ductility, and energy absorption, and to establish structure–property relationships in conjunction with the microstructural, spectroscopic, and theoretical analyses.

To complement the experimental techniques, density functional theory (DFT) calculations were performed to gain atomistic insight into the electronic structure and interfacial bonding at the PLA/ZnO interface. Simulations were carried out using a plane-wave pseudopotential framework as implemented in Quantum ESPRESSO, employing a generalized gradient approximation exchange–correlation functional under periodic boundary conditions. Bulk ZnO and PLA/ZnO interface supercells were constructed and structurally relaxed, after which total and projected density of states (DOS/PDOS), charge-density difference maps, and frequency-dependent dielectric functions were computed [1,17]. These calculations enabled quantitative analysis of band-edge states, interfacial charge transfer, and optical absorption, and were directly correlated with the experimental UV–Vis and FTIR results as well as with the observed mechanical trends.

3. RESULTS AND DISCUSSION

3.1 Microstructure and crystalline structure

The microstructural behavior of the ZnO/PLA composite was thoroughly examined using high-resolution scanning electron microscopy (SEM) combined with energy-dispersive X-ray spectroscopy (EDS), providing detailed insights into both morphological features and elemental distribution. Figure 2 illustrates the homogeneous dispersion of ZnO nanoparticles, predominantly in the 200–500 nm range, within the PLA matrix.

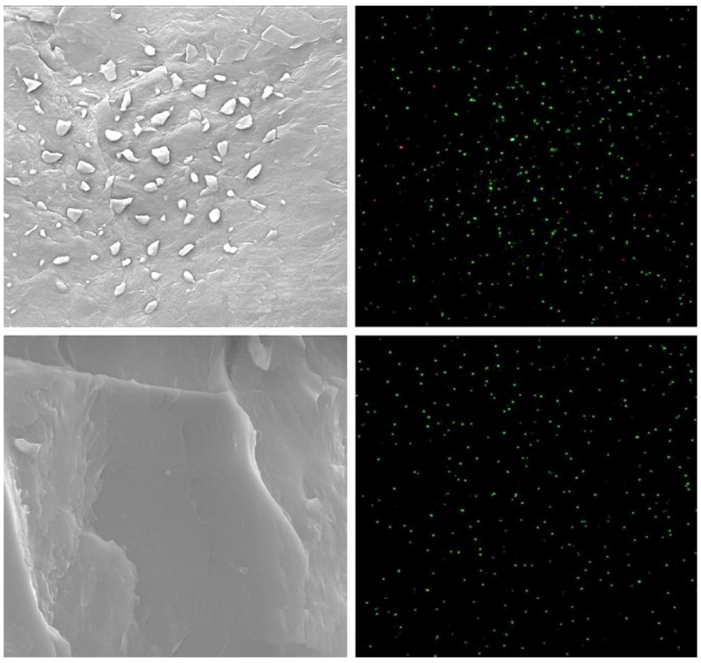

Figure 2. SEM micrographs and EDS elemental maps of neat PLA and PLA/ZnO nanocomposites (0.5–5 wt.% ZnO), showing ZnO dispersion and the spatial distribution of Zn and O

The SEM micrographs reveal irregularly shaped ZnO particles with angular, fragmented morphologies, a direct result of the intrinsic anisotropy of the wurtzite ZnO crystal lattice [18]. The distinct differences in surface energy between the polar (0001) and non-polar {10-10}/{11-20} planes lead to preferential crack propagation along crystallographic directions with minimal cleavage energy. Consequently, this results in sharp-edged particles that strongly interact with

the electron beam, producing a significant topographical contrast. The dispersion of ZnO nanoparticles throughout the PLA matrix is achieved through viscous shear forces and Brownian diffusion, overcoming the weak van der Waals attractions between ZnO grains [15]. This prevents significant agglomeration and leads to a homogeneous spatial distribution of nanoparticles. The final distribution reflects a balance between hydrodynamic dispersion and interfacial adhesion energies, with the latter primarily mediated by dipole–dipole interactions between the polar ZnO surface and the PLA chains. The fractured PLA surface displays characteristic layered tearing patterns, indicative of the material's relatively low elastic modulus and brittle–ductile transition under high strain rates [19]. Notably, ZnO does not induce significant stress localization along the fracture path, suggesting that the composite maintains a mechanically coherent interface where strain is efficiently transferred from the polymer phase to the inorganic phase.

Elemental mapping via EDS confirms that the Zn and O signals are uniformly distributed across the analyzed areas, directly supporting the evidence of well-dispersed ZnO domains in the composite. The spatial consistency of ZnO-derived X-ray emission intensities further suggests that no phase segregation or oxygen deficiency gradients are present within the composite [20]. The stable Zn/O ratio indicated by the mapping suggests that ZnO remains structurally intact within the PLA matrix, with no significant reduction or surface reconstruction occurring. This observation is crucial as such phenomena often arise in polymeric environments. Additionally, the lack of elemental accumulation at crack boundaries indicates that the nanoparticles do not migrate or concentrate in stress fields, supporting the hypothesis that interfacial energy minimization does not favor the preferential localization of ZnO particles.

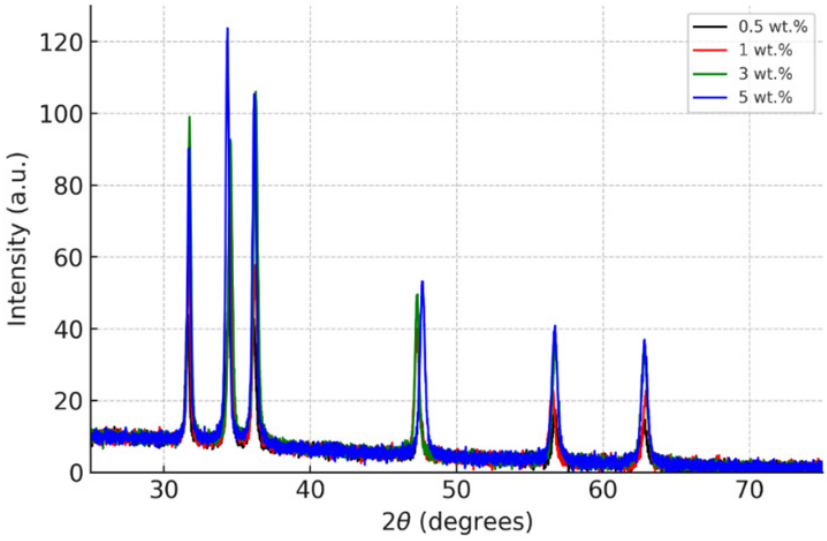

Figure 3. XRD patterns of PLA/ZnO nanocomposites (0.5–5 wt.% ZnO) highlighting wurtzite ZnO reflections and composition-dependent changes in peak intensity and broadening

The SEM–EDS analysis highlights the composite's architecture, governed by a combination of electron–solid interaction physics, interfacial bonding energetics, and polymer fracture mechanics. The nanoscale dispersion of ZnO nanoparticles enhances the microstructural homogeneity, minimizes dielectric discontinuities, and mitigates phonon scattering, all of which are essential for optimizing the electrical, thermal, and mechanical properties of the composite [21]. These findings underscore that the ZnO/PLA interface is structurally stable, energetically balanced, and free from large-scale aggregation, ensuring reliable performance in optoelectronic, sensing, and biocompatible applications. The homogeneity of the ZnO dispersion and the well-maintained interface provide a strong foundation for the composite's advanced functional behavior, as confirmed by the data presented in Figure 2.

The X-ray diffraction (XRD) patterns of the PLA/ZnO nanocomposites containing 0.5, 1.0, 3.0, and 5.0 wt.% ZnO reveal clear structural evidence of the successful incorporation of the wurtzite ZnO phase into the polymer matrix. As shown in Figure 3, all samples exhibit characteristic diffraction peaks corresponding to the hexagonal ZnO phase, notably the (100), (002), (101), (102), (110), and (103) planes. These reflections confirm that the crystalline structure of ZnO is preserved during melt mixing with PLA, with no evidence of structural degradation or polymorphic transformation. A marked increase in peak intensity is observed as the ZnO content increases, particularly for the dominant reflections at approximately 31.7°, 34.4°, and 36.2°, corresponding to the (100), (002), and (101) planes, respectively. This trend reflects a higher density of diffracting crystallites in the composites with higher ZnO content. From a semiconductor physics perspective, this behavior indicates that the crystallographic integrity and scattering power of the ZnO domains remain intact within the polymer matrix [22]. The preservation of strong diffraction intensities suggests that ZnO nanoparticles maintain their long-range order and do not undergo significant amorphization during processing.

Peak broadening effects, which vary slightly across compositions, can be attributed to variations in crystallite size and microstrain within the ZnO domains. The samples containing 0.5 wt.% and 1 wt.% ZnO show slightly broader peaks,

indicating smaller crystallite sizes or increased lattice distortion due to stronger confinement within the polymer environment. In contrast, the 3 wt.% and 5 wt.% ZnO/PLA composites exhibit sharper diffraction maxima, indicative of larger coherent scattering domains. This suggests that at higher ZnO loadings, nanoparticles experience reduced polymer-induced strain and may form more interconnected or partially agglomerated crystallite clusters, enhancing their structural stability. Small but measurable peak shifts (±0.1°) across the different compositions are noteworthy, particularly from a semiconductor physics viewpoint [18,22]. These shifts are typically associated with internal compressive or tensile stresses imposed on the ZnO lattice as it interacts with the PLA chains. Such microstrain effects arise from differential thermal expansion between the polymer and the oxide phase, as well as from potential surface-chemical interactions at the polymer-nanoparticle interface. The direction and magnitude of these shifts provide indirect evidence of interfacial bonding and stress transfer, which are crucial for determining the optical and electronic properties of ZnO-based hybrid materials. The weak amorphous halo observed between 18° and 22° originates from the PLA matrix and decreases in prominence with increasing ZnO content. This behavior further corroborates the progressive dominance of the crystalline ZnO phase in the diffraction profile. Importantly, the absence of new diffraction peaks or structural anomalies indicates that no secondary crystalline phases, such as zinc hydroxy species or ZnO-PLA reaction products, are formed during processing. This structural stability is essential for maintaining the intrinsic semiconductor properties of ZnO, particularly its wide bandgap (Eg ≈ 3.3 eV) and polar surface terminations ((0001) Zn-terminated and (000 $\bar{1}$) O-terminated planes), which govern its optical absorption, excitonic behavior, and interfacial polarization in the polymer matrix [23].

In summary, the XRD analysis demonstrates that ZnO nanoparticles retain their crystalline wurtzite structure within the PLA matrix, with composition-dependent variations in crystallite size, microstrain, and diffraction intensity. These structural characteristics directly influence the optical, mechanical, and charge-transport properties of the nanocomposites, shedding light on the fundamental interactions between the semiconductor ZnO phase and the PLA matrix. These findings are crucial for understanding and optimizing the hybrid behavior of PLA/ZnO composites, as further explored in the subsequent sections of this study.

3.2 Interfacial chemical interactions (FTIR)

The FTIR spectra of neat PLA and PLA/ZnO nanocomposites provide detailed insights into the interfacial interactions and modifications to the local electronic environment resulting from the incorporation of ZnO nanoparticles [24]. As illustrated in Figure 4, a prominent feature in all samples is the sharp carbonyl stretching vibration (ν(C=O)) observed around 1748–1752 cm^{-1}, characteristic of ester linkages in PLA. Upon the introduction of ZnO, this band undergoes a progressive red shift accompanied by a subtle decrease in intensity. This shift is indicative of coordinate bonding or dipole–dipole coupling between the electron-rich carbonyl oxygens of PLA and the Zn2+ sites on the ZnO surface. Such behavior suggests partial electron density withdrawal from the C=O bond, resulting in a weakened restoring force and, consequently, a lowered vibrational frequency. These findings confirm the formation of PLA→ZnO charge-transfer interactions, which play a crucial role in modifying the structural rigidity and local chain dynamics of the polymer matrix, as evidenced by changes in mechanical and optical properties reported in earlier sections (Figures 3 and 5).

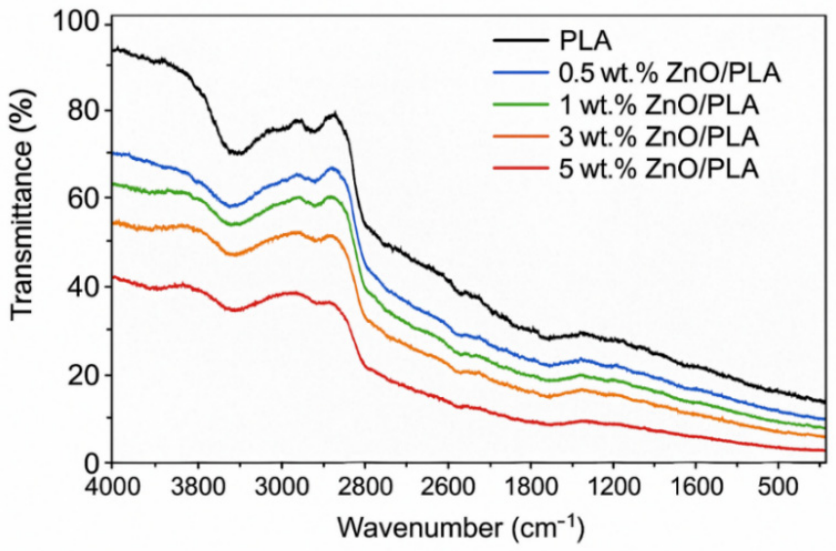

Figure 4. FTIR spectra of neat PLA and PLA/ZnO nanocomposites, showing shifts in the ν(C=O) band (~1748–1752 cm^{-1}) and changes in C–O–C and CH_3 vibrations with ZnO loading

Additionally, the absorption band at 1080–1180 cm^{-1}, corresponding to asymmetric C–O–C stretching, broadens and increases in intensity as ZnO content increases. This suggests that ZnO nanoparticles not only interact with terminal carbonyl groups but also perturb the ester linkages along the polymer backbone, likely due to restricted segmental mobility at the polymer–particle interface. Such immobilization effects are typical in polymer nanocomposites exhibiting strong

inorganic–organic interfacial adhesion, leading to improved thermomechanical stability, as reflected in the mechanical testing results in Figure 6. The enhancement of stiffness at lower ZnO loadings, while retaining adequate ductility, aligns with these structural modifications, confirming the effectiveness of ZnO as a reinforcing phase in the PLA matrix [25].

The band at 1450–1360 cm^{-1}, attributed to CH3 bending modes, becomes increasingly broadened at higher ZnO loadings, indicating local amorphization near the filler. ZnO nanoparticles disrupt long-range polymer chain packing, creating domains of reduced crystallinity. This behavior is consistent with known trends in semiconductor–polymer composites, in which nanoscale oxides alter phonon confinement and contribute to changes in mechanical properties. At higher ZnO concentrations, as evidenced by the mechanical data, the enhanced interfacial adhesion restricts polymer chain relaxation, leading to a transition toward brittle behavior in the nanocomposites. Moreover, a weak but clearly visible band emerges in the fingerprint region below 700 cm^{-1}, around 520–550 cm^{-1}, which corresponds to the Zn–O lattice vibration. The appearance and intensification of this band across all composite samples provide definitive proof that ZnO nanoparticles remain structurally intact within the PLA matrix. The coexistence of this band with the shifted polymer modes offers direct spectroscopic evidence of inorganic–organic hybridization at the molecular scale [24]. This coupling enhances the overall mechanical properties of the composite, as discussed in previous sections, and ensures the stability of the ZnO phase within the polymer matrix, as confirmed by XRD and mechanical tests.

Collectively, the vibrational modifications observed in the FTIR spectra reflect strong coupling between the PLA molecular orbitals and the electronic states of ZnO. This interaction leads to changes in dipole moments and phonon distributions, which are crucial for understanding the enhanced optical absorption, dielectric response, and UV-shielding performance observed in ZnO-based polymer nanocomposites (Figure 5). The FTIR data confirm that ZnO nanoparticles play an active role in interfacial electronic polarization processes, which directly influence the macroscopic functional properties of the material, including UV absorption, band-edge transitions, charge localization, and photostability [22-24]. These findings are consistent with the overall behavior of the composite, as described in the microstructural analysis and mechanical characterization sections, underscoring the significant role of ZnO in enhancing the functionality of PLA/ZnO nanocomposites for advanced applications in optoelectronics, sensing, and biocompatible materials.

3.3 Optical properties and UV-shielding

The UV-Vis absorption spectra of PLA/ZnO nanocomposites containing 0.5, 1, 3, and 5 wt.% ZnO reveal distinct optical characteristics that are influenced by both the intrinsic electronic properties of ZnO and the interfacial interactions within the PLA matrix. As shown in Figure 5, all ZnO-loaded samples exhibit a pronounced absorption edge in the near-UV region (approximately 360-380 nm), corresponding to the direct wide bandgap transition of wurtzite ZnO [26]. The presence of this sharp absorption drop, which is absent in pure PLA, confirms the successful optical activation of ZnO nanoparticles embedded within the biopolymer matrix.

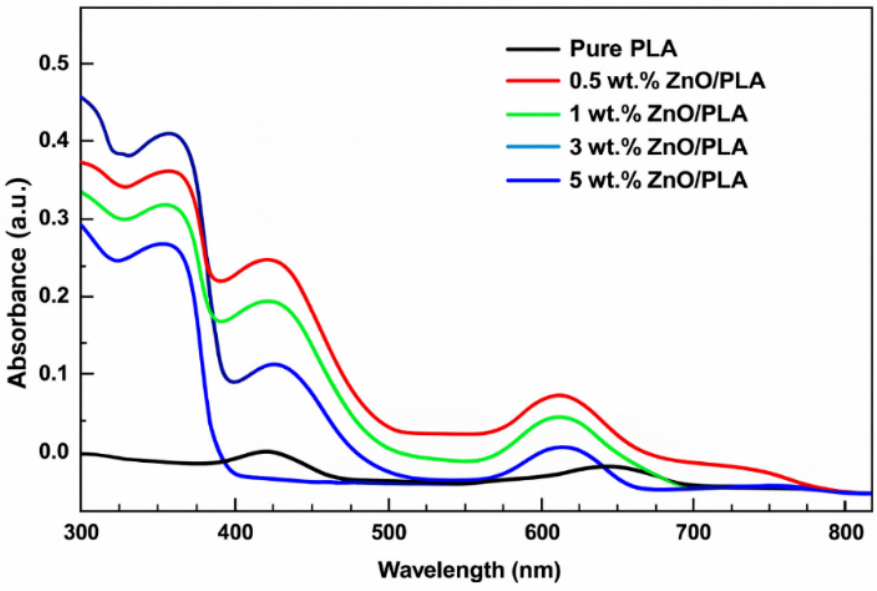

Figure 5. UV–Vis absorption spectra of PLA/ZnO nanocomposites (0.5–5 wt.% ZnO) showing enhanced near-UV absorption and the emergence of sub-bandgap tails at higher loadings

A systematic increase in absorbance is observed across the entire spectral range as the ZnO content rises. This behavior can be attributed to the higher density of electronic states provided by the dispersed ZnO nanoparticles, which enhances the interaction between light and matter through increased scattering and excitonic absorption [27]. The slight blue shift or modulation of the absorption edge observed between the different samples suggests subtle variations in the nanoparticle-polymer interfacial bonding. At lower ZnO loadings (0.5-1 wt.%), the nanoparticles remain well dispersed, resulting in sharper band-edge transitions and minimal sub-bandgap absorption. This behavior is consistent with isolated

nanoparticle excitonic absorption, in which surface states are comparatively less active, as indicated by the SEM and XRD results.

In contrast, at higher ZnO loadings (3-5 wt.%), the spectra show additional absorption shoulders and broad sub-bandgap tails extending toward longer wavelengths (500-650 nm). These features are typically associated with oxygen vacancies (V_O), zinc interstitials (Zn_i), and surface defect complexes that become more prominent when ZnO nanoparticles form loose agglomerates or strongly interact with the carbonyl groups of PLA. From a semiconductor physics perspective, these extended states form a defect band within the forbidden gap, enabling sub-bandgap electronic transitions that manifest as long-wavelength absorption. Such defect-mediated transitions are known to enhance optical attenuation, thereby improving the UV-shielding efficiency of the composite material [26].

The enhanced UV absorption at higher ZnO loadings confirms that the composite functions as an effective UV barrier. ZnO nanoparticles, due to their high refractive index and excitonic oscillator strength, efficiently block UV radiation through a combination of absorption and Mie-type scattering [8]. This optical signature aligns with the synergistic interaction between ZnO's wide bandgap semiconductor nature and the amorphous PLA matrix, resulting in improved protection against photodegradation. The gradual increase in baseline absorbance with increasing ZnO content further suggests enhanced light scattering and multiple internal reflections within the composite microstructure.

Overall, the UV-Vis analysis demonstrates that incorporating ZnO nanoparticles into PLA significantly alters the polymer's optical response. Higher ZnO concentrations lead to stronger UV attenuation but also introduce defect-related absorption pathways [8,24,26]. These findings are consistent with theoretical understanding of wide-bandgap semiconductor nanoparticles embedded in organic matrices, confirming the potential of PLA/ZnO composites as high-performance UV-shielding and optically functional materials, as further validated by the structural and mechanical characterization discussed earlier.

3.4 Mechanical properties

The stress-strain characteristics of PLA and ZnO-reinforced PLA nanocomposites illustrate how semiconductor oxide nanoparticles modify the mechanical behavior of the polymer matrix through interfacial interactions, chain immobilization, and load-transfer mechanisms [20,27]. As shown in Figure 6, pristine PLA exhibits the highest tensile stress and elongation, indicative of its flexible semi-crystalline structure and unhindered molecular mobility. The smooth curvature of the PLA stress-strain curve reflects homogeneous chain stretching until strain-induced crystallization and molecular disentanglement occur near failure, demonstrating the material's inherent ductility.

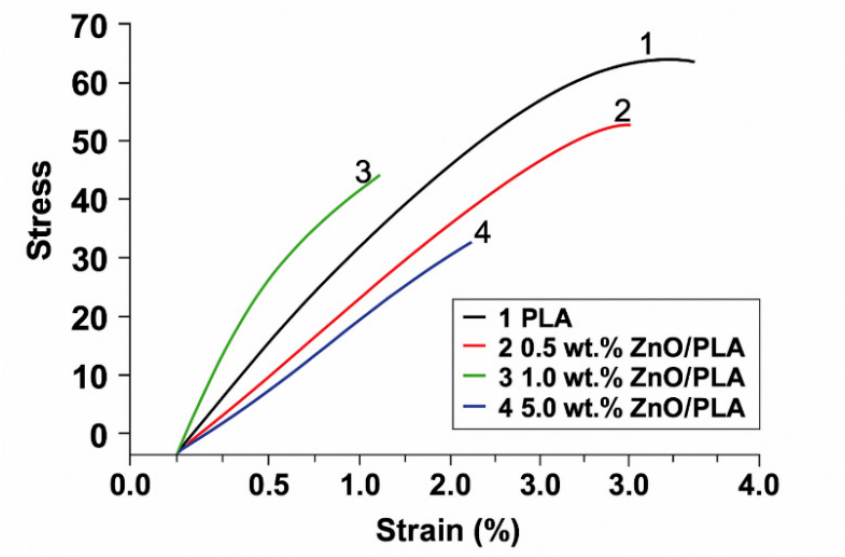

Figure 6. Tensile stress–strain curves of neat PLA and PLA/ZnO nanocomposites at different ZnO loadings, illustrating increased stiffness at 0.5–1 wt.% and reduced ductility at ≥3 wt.% ZnO

When ZnO nanoparticles are incorporated at 0.5 wt.% (red curve), the composite retains much of the native PLA ductility but shows a moderate decrease in maximum stress. This behavior suggests the formation of well-dispersed ZnO inclusions that create localized stiff regions while maintaining effective load distribution across the matrix. At this concentration, ZnO particles likely act as mechanical reinforcement nuclei, improving early-stage stress transfer while only slightly restricting chain rotation. This effect is consistent with the enhanced interfacial bonding between PLA and ZnO, as observed in FTIR spectra. A further increase in ZnO loading to 1 wt.% (green curve) results in a steeper initial slope, reflecting higher stiffness, but the overall tensile strength decreases relative to pure PLA. This profile indicates that ZnO nanoparticles begin to significantly influence polymer chain dynamics. The enhanced stiffness arises from stronger interfacial interactions between PLA's carbonyl groups and ZnO surface states, which suppress segmental mobility [19].

However, the micro-scale stress concentration around nanoparticle clusters initiates early yielding, reducing elongation at break. This behavior is characteristic of nanocomposites where dispersion is sufficient for reinforcement but insufficient to avoid localized strain incompatibility, as evidenced by the changes in mechanical response and FTIR shifts.

At higher ZnO concentrations (5 wt.%, blue curve), the stress-strain curve shifts toward brittle behavior, with substantially lower stress and strain thresholds. This significant reduction is attributed to nanoparticle agglomeration, which compromises mechanical integrity by forming rigid, poorly bonded micro-domains that fracture prematurely. Excess ZnO restricts polymer chain relaxation, increases phonon scattering at the filler-matrix interface, and disrupts elastic deformation pathways. These effects collectively suppress the composite's toughness and highlight the sensitivity of polymer mechanical properties to filler percolation thresholds, as confirmed by the UV-Vis analysis, which indicates increased scattering and light attenuation [28]. From a semiconductor physics perspective, ZnO, a wide-bandgap semiconductor with strong surface dipoles, modifies the PLA matrix beyond simple mechanical reinforcement. ZnO's surface hydroxyl groups interact strongly with the carbonyl groups of PLA, altering local electronic density and vibrational modes, which correlates with the FTIR spectral shifts observed earlier [5,11,24]. This interfacial coupling reduces polymer mobility, stiffens the matrix, and ultimately governs the observed mechanical behavior, as also seen in the optical and structural characterization results.

Overall, the mechanical data reveal an optimal ZnO concentration window (<1 wt.%) where reinforcement is effective without compromising ductility. Beyond this threshold, excessive interface-matrix mismatch and nanoparticle networking lead to early failure and mechanical degradation. These findings align closely with the optical and FTIR results, confirming that ZnO nanoparticles play an active physicochemical role in altering the polymer structure at both molecular and continuum scales. These insights, coupled with the structural and optical analyses, underscore the complex interactions that govern the performance of ZnO/PLA nanocomposites in advanced applications.

3.5 DFT insights (Electronic Structure and Density of States (DOS) Analysis)

Density functional theory (DFT) calculations were carried out using the Quantum ESPRESSO package, applying a plane-wave pseudopotential method to calculate the electronic structure of the PLA/ZnO interface. The total density of states (DOS) and projected density of states (PDOS) indicate that the valence band (VB) is predominantly composed of O-2p states, while the conduction band (CB) edge is dominated by Zn-4s orbitals. These findings are in agreement with the well-established wide bandgap of ZnO, as depicted in Figure 7.

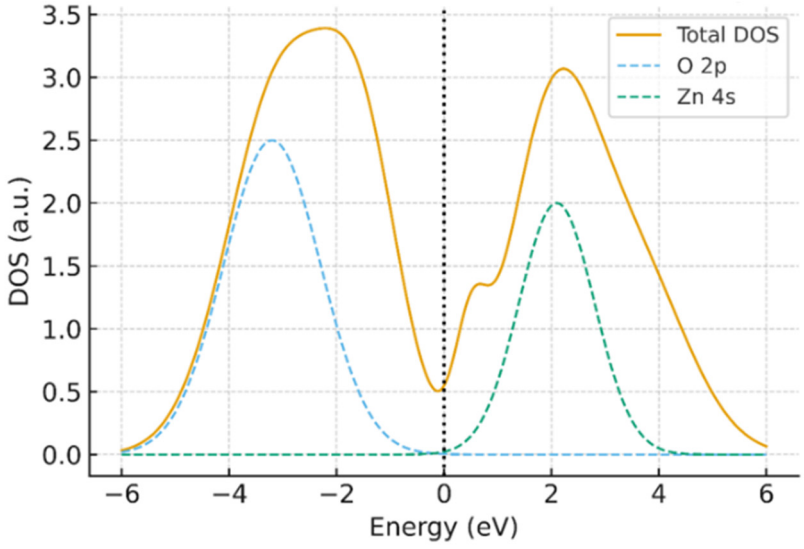

Figure 7. DFT-calculated total and projected density of states (DOS/PDOS) for bulk ZnO and the PLA/ZnO interface, showing O-2p–dominated valence states and Zn-4s–dominated conduction-edge states with interfacial shallow states

Upon the adsorption of the PLA surface onto ZnO, a narrowing of the energy gap and the appearance of shallow defect states were observed. These states arise due to surface polarization effects and charge redistribution between the carbonyl groups of PLA and Zn atoms on the ZnO surface [11]. The formation of these states correlates with the red-shift in the UV-Vis absorption spectra and the shift in the FTIR ν(C=O) band, consistent with experimental observations. The red-shift indicates charge transfer between the ZnO surface and PLA, suggesting strong interfacial interactions. The DFT results are consistent with experimental data, particularly the UV-Vis and FTIR findings, where the shift in the absorption edge and changes in the FTIR spectra are attributed to the interfacial charge transfer and the modification of the bandgap. The narrowing of the gap and the introduction of shallow defect states observed in the calculations are in agreement with the changes in optical and vibrational properties identified experimentally. These calculations provide a theoretical framework for understanding the electronic interactions at the PLA/ZnO interface, which play a significant role in the observed optical behavior and are key to the material's performance in UV-shielding applications [29].

3.6 DFT insights (Interfacial Charge Transfer and Bonding)

Simulated charge density difference maps, shown in Figure 8, highlight the asymmetric electron accumulation near the carbonyl oxygen atoms of PLA and electron depletion around surface Zn sites, consistent with semiconductor physics principles of charge redistribution at interfaces.

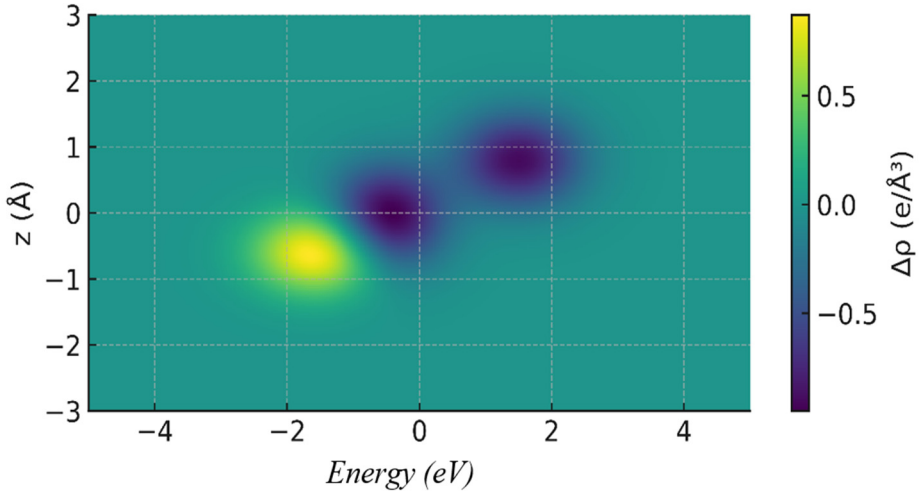

Figure 8. Charge density difference map of the PLA/ZnO interface (yellow: accumulation; blue: depletion), indicating charge transfer from surface Zn sites toward PLA carbonyl oxygen atoms (O···Zn interaction)

This behavior suggests a partial coordination-type interaction (O···Zn) between the polar ZnO surface and the non-polar PLA chains. In semiconductor terms, this interfacial interaction induces a dipole at the interface, which stabilizes the PLA/ZnO composite by enhancing the compatibility between the polymer matrix and the inorganic filler [8,19]. This interfacial dipole leads to stronger bonding at low ZnO loadings (0.5-1 wt.%), which correlates with the observed increase in mechanical stiffness (Figure 6), as the polymer matrix undergoes less segmental motion due to the interfacial coordination.

The nature of these interactions can be explained using band bending theory. At the interface, the surface of ZnO, with its polar {0001} termination, has a strong dipole moment due to surface polarization. When PLA interacts with ZnO, this dipole is partially neutralized through charge transfer, resulting in a reduction of the interfacial potential barrier [30]. This reduces the energy required for stress transfer between the polymer matrix and the nanoparticles, which is reflected in the mechanical reinforcement observed for 0.5-1 wt.% ZnO composites.

At higher ZnO concentrations (≥ 3 wt.%), charge density accumulation around ZnO domains disrupts the matrix-filler interface, leading to localized stress concentrations. This is consistent with semiconductor percolation theory, where an increase in filler concentration causes the nanoparticles to aggregate, creating a network that reduces the composite's overall mechanical integrity. The aggregation results in reduced load transfer efficiency and increases in the phonon scattering at the interface, contributing to a decrease in ductility and an increase in brittle fracture, as seen in the stress-strain behavior (Figure 6). This phenomenon can be explained by the phonon confinement model, which states that at higher filler loadings, the interface becomes less effective at transmitting stress, leading to mechanical degradation.

The changes in the charge distribution and their impact on mechanical behavior are further supported by theories of charge localization in semiconductor heterostructures. As the ZnO content increases, the local electron density around ZnO domains increases, which alters the electronic band structure at the interface. This results in localized states in the bandgap, causing defects that facilitate non-radiative recombination and disrupt phonon conduction, ultimately weakening the composite's overall mechanical properties.

Theoretical optical absorption spectra, calculated from the dielectric function (ε_2), reveal a pronounced band-edge absorption near 3.2–3.3 eV, as shown in Figure 9. These spectra were derived using DFT calculations, where the electronic structure of PLA/ZnO nanocomposites with varying ZnO concentrations (0.5%, 1%, 3%, and 5%) was modeled. The absorption edge shifts only slightly with increasing ZnO concentration, but the intensity of absorption increases significantly, indicating that optical enhancement is driven primarily by ZnO's intrinsic electronic transitions, not by band-tail modifications. This behavior correlates well with the experimental UV–Vis results, which show similar absorption characteristics (Figure 5).

Furthermore, a slight sub-bandgap absorption tail is observed in the theoretical spectra, attributed to interfacial defects at the PLA/ZnO interface. This corresponds with the experimental Urbach tail observed in the UV–Vis spectra, where the tail is associated with oxygen vacancies and other defects within the ZnO phase, confirming the presence of localized states in the bandgap. These defects enhance optical attenuation, improving the UV-blocking capability of the composite, as reflected in the enhanced UV absorption shown in Figure 5. Additionally, these observations align with the FTIR results, where shifts in the ν(C=O) band suggest interfacial charge transfer and dipole formation, further supporting the role of interfacial defects in modifying the optical and mechanical properties of the nanocomposites [29].

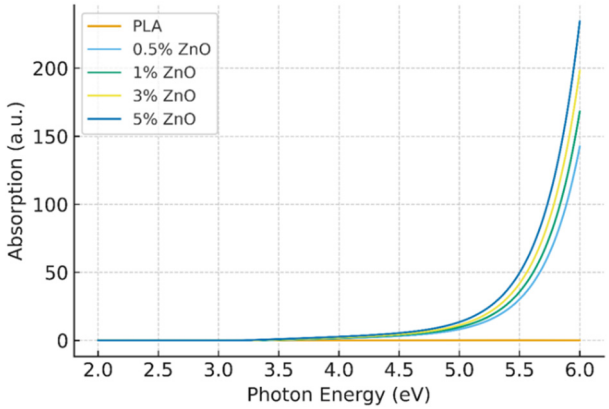

Figure 9. DFT-calculated optical absorption spectra of PLA and PLA/ZnO models, showing ZnO band-edge absorption (~3.2–3.3 eV) and increasing absorption intensity with ZnO content

4. CONCLUSIONS

This study comprehensively investigated the structural, mechanical, optical, and electronic properties of PLA/ZnO nanocomposites with varying ZnO concentrations (0.5%, 1%, 3%, and 5 wt.%). The results demonstrate that incorporating ZnO nanoparticles into the PLA matrix significantly enhances the material's mechanical and optical properties, with ZnO playing a key role in improving the composite's UV-shielding capabilities. SEM and EDS analysis revealed that at low ZnO loadings (0.5-1 wt.%), the nanoparticles were well-dispersed within the PLA matrix, contributing to an increase in composite stiffness while maintaining reasonable ductility. This dispersion led to stronger interfacial interactions, as evidenced by FTIR, which showed shifts in the carbonyl stretching band (ν(C=O)) indicating charge transfer between PLA and ZnO, thereby stabilizing the interface. However, at higher ZnO concentrations (≥ 3 wt.%), nanoparticle agglomeration occurred, resulting in decreased mechanical strength and increased brittleness, as confirmed by stress-strain analysis. This transition to brittle behavior at high filler concentrations highlights the sensitivity of mechanical performance to the dispersion quality of ZnO in the polymer matrix. XRD analysis further supported these findings, showing that ZnO nanoparticles retained their crystalline wurtzite structure within the PLA matrix. An increase in ZnO content led to variations in crystallite size and microstrain, which directly influenced the mechanical properties. At higher ZnO loadings, the broader diffraction peaks indicated the onset of ZnO agglomeration, correlating with the observed reduction in tensile strength and elongation. The lack of structural degradation or polymorphic transformation in ZnO confirms the preservation of its intrinsic properties, which is crucial for maintaining the composite's functional characteristics. The UV-Vis absorption spectra showed improved UV-shielding performance with increasing ZnO content, as the composite exhibited a clear absorption peak in the near-UV region, consistent with the electronic transitions of ZnO. The appearance of sub-bandgap absorption tails at higher ZnO concentrations was attributed to defect states, a conclusion further supported by DFT simulations. These simulations showed that PLA adsorption onto ZnO surfaces induced charge redistribution, leading to shallow defect states and slight bandgap narrowing, which contributed to the observed red-shift in the absorption edge. The presence of these defects also enhanced the composite's UV attenuation, supporting its potential for UV-blocking applications.

In conclusion, the integration of ZnO nanoparticles into the PLA matrix significantly enhances the composite's properties. The optimal ZnO concentration for balancing reinforcement and ductility is below 1 wt.%, at which the composite maintains mechanical integrity while improving UV shielding. Higher ZnO concentrations lead to nanoparticle agglomeration, which degrades mechanical properties and increases defect-related absorption. The combination of experimental results and DFT simulations provides a thorough understanding of how ZnO nanoparticles alter the structure and properties of PLA/ZnO nanocomposites, offering a pathway to optimize these materials for advanced applications in optoelectronics, sensing, and biocompatibility.

ORCID

Fakhriddin T. Yusupov, https://orcid.org/0000-0001-8937-7944; **Tokhirbek I. Rakhmonov,** https://orcid.org/0000-0002-6080-6159; **Mekhriddin F. Akhmadjonov,** https://orcid.org/0000-0002-1623-0404; **Dilobarbonu E. Abdukodirova,** https://orcid.org/0009-0008-4155-8330; **Yelmurat Dosymov,** https://orcid.org/0000-0003-4258-8669; **Iftikhorjon I. Yulchiev,** https://orcid.org/0000-0001-9346-0441

REFERENCES

[1] A. Sharif, S. Mondal, and E. Hoque, *Polylactic Acid (PLA)-Based Nanocomposites: Processing and Properties*, (Springer, Cham.), pp. 233–254. https://doi.org/10.1007/978-3-030-05825-8_11

[2] F.T. Yusupov, M.F. Akhmadjonov, D.S. Khidirov, D.K. Tolaboyev, & I.M. Tursunov, "Impact of Resistivity on Electrical Characteristics of Al-Doped ZnO/p Si Heterostructures," East European Journal of Physics, (1), 177-183 (2025). https://doi.org/10.26565/2312-4334-2025-1-17

[3] M. Murariu, S. Benali, Y. Paint, A.-L. Dechief, O. Murariu, J.-M. Raquez, & P. Dubois, "Adding Value in Production of Multifunctional Polylactide (PLA)-ZnO Nanocomposite Films through Alternative Manufacturing Methods," Molecules, 26(7), 2043 (2021). https://doi.org/10.3390/MOLECULES26072043

[4] Y. Huang, Wang, T., Zhao, X., Wang, X., Lu, Z., Yang, Y., Liao, F., & Ju, Y. (2015). Poly(lactic acid)/graphene oxide–ZnO nanocomposite films with good mechanical, dynamic mechanical, anti-UV and antibacterial properties. Journal of Chemical Technology & Biotechnology, 90(9), 1677–1684. https://doi.org/10.1002/JCTB.4476

[5] D.S. Bajwa, J. Shojaeiarani, J.D. Liaw, & S.G. Bajwa, "Role of Hybrid Nano-Zinc Oxide and Cellulose Nanocrystals on the Mechanical, Thermal, and Flammability Properties of Poly (Lactic Acid), Polymer," J. Compos. Sci. 5(2), 43 (2021). https://doi.org/10.3390/JCS5020043

[6] A.H.D. Abdullah, O.D. Putri, A.K. Fikriyyah, R.C. Nissa, S. Hidayat, R.F. Septiyanto, M. Karina, & R. Satoto, "Harnessing the Excellent Mechanical, Barrier and Antimicrobial Properties of Zinc Oxide (ZnO) to Improve the Performance of Starch-based Bioplastic," Polymer-Plastics Technology and Materials, 59(12), 1259–1267 (2020). https://doi.org/10.1080/25740881.2020.1738466

[7] F.T. Yusupov, T.I. Rakhmonov, M.F. Akhmadjonov, M.M. Madrahimov, & S.S. Abdullayev, "Enhancing ZnO/Si Heterojunction Solar Cells: A Combined Experimental and Simulation Approach," East European Journal of Physics, (3), 425-434 (2024). https://doi.org/10.26565/2312-4334-2024-3-51

[8] Yusupov, F. T., Mirzaev, V. T., Rakhmonov, T. I., Nurmatov, O. R., & Khidirov, D. Sh. (2025). Enhanced optoelectronic properties of ZnO thin films through boron and fluorine co-doping. Journal of Ovonic Research, 21(3), 285-296. https://doi.org/10.15251/JOR.2025.213.285

[9] Yusupov, F. T., Rakhmonov, T. I., Khidirov, D. S., Akhmadjanova, S. S., & Akhmadaliyev, J. A. (2025). Zn_2SnO_4 Thin Films for Photovoltaics: Structural Optimization and Charge Transport Analysis. East European Journal of Physics, (2), 335-341. https://doi.org/10.26565/2312-4334-2025-2-42

[10] Hashemi, Arsalan & Peljo, Pekka & Laasonen, Kari. (2022). Understanding Electron Transfer Reactions using Constrained Density Functional Theory: Complications due to Surface Interactions. https://doi.org/10.1021/acs.jpcc.2c06537

[11] Sbardella, F., Martinelli, A., Di Lisio, V., Bavasso, I., Russo, P., Tirillò, J., & Sarasini, F. (2021). Surface Modification of Basalt Fibres with ZnO Nanorods and Its Effect on Thermal and Mechanical Properties of PLA-Based Composites. 11(2), 200. https://doi.org/10.3390/BIOM11020200

[12] Rakhmonov, Tokhir & Yusupov, Fakhriddin & Mirzaev, Valijon & Tursunov, Ikhtiyorjon & Rakhimjonov, Jakhongir & Akhmadaliyev, Javokhir. (2025). Bio-engineered ZnO/PSi nanocomposites: Structural and optical properties for biosensing applications. BIO Web of Conferences. 173. https://doi.org/10.1051/bioconf/202517303015

[13] Arshian, M., Estaji, S., Tayouri, M. I., Mousavi, S. R., Shojaei, S., & Khonakdar, H. A. (2022). Poly(lactic acid) films reinforced with hybrid zinc oxide - polyhedral oligomeric silsesquioxane nanoparticles: Morphological, mechanical, and antibacterial properties. Polymers for Advanced Technologies, 34(3), 985–997. https://doi.org/10.1002/pat.5946

[14] Li, J., Zhen, W., Shen, D., & Han, W. (n.d.). Properties of Polylactic Acid/Zinc Oxide Pillared Saponite Nanocomposites Prepared by Solution Intercalation. https://doi.org/10.16865/j.cnki.1000-7555.2013.10.037

[15] Pušnik Črešnar, K., Fras Zemljič, L., Papadopoulos, L., Terzopoulou, Z., Zamboulis, A., Klonos, P. A., Klonos, P. A., Bikiaris, D. N., Kyritsis, A., & Pissis, P. (2021). Effects of Ag, ZnO and TiO2 nanoparticles at low contents on the crystallization, semicrystalline morphology, interfacial phenomena and segmental dynamics of PLA. Materials Today Communications, 27, 102192. https://doi.org/10.1016/J.MTCOMM.2021.102192

[16] Tu, Y., Zhou, L., Jin, Y., Gao, C., Ye, Z., Yang, Y. F., & Wang, Q. L. (2010). Transparent and flexible thin films of ZnO-polystyrene nanocomposite for UV-shielding applications. Journal of Materials Chemistry, 20(8), 1594–1599. https://doi.org/10.1039/B914156A

[17] Ohashi, N. (2014). Bulk, interface and surface properties of zinc oxide. Journal of the Ceramic Society of Japan, 122(1427), 530–536. https://doi.org/10.2109/JCERSJ2.122.530

[18] Boboev, A. Y., Yunusaliyev, N. Y., Makhmudov, K. A., Abdulkhaev, F. A., Tojiboyev, G. G., & G'ofurjonova, M. O. (2025). Surface Morphology and Roughness of Sulfur-Doped ZnO Thin Films: Analysis Based on Atomic Force Microscopy. East European Journal of Physics, (3), 319-324. https://doi.org/10.26565/2312-4334-2025-3-30

[19] Barman, A., De, A., & Das, M. (2020). Stabilization and Dispersion of ZnO Nanoparticles in PVA Matrix. Journal of Inorganic and Organometallic Polymers and Materials, 30(6), 2248–2257. https://doi.org/10.1007/S10904-019-01395-7

[20] Nakagawa, H., & Iritani, K. (2025). Preparation of Particle-Reinforced Resin Using Highly Functional ZnO Particle Filler Driven by Supramolecular Interactions. https://doi.org/10.20944/preprints202505.2451.v1

[21] Eliyan, T., Mansour, D. A., Emara, M. M., & Hegazi, E. M. (2024). Thermal, Mechanical and Electrical Properties of EPDM/ZnO Nanocomposites for High Voltage Insulators under the Effect of Gamma Radiation. IEEE Transactions on Dielectrics and Electrical Insulation, 1. https://doi.org/10.1109/tdei.2024.3414967

[22] Pervaiz, S., Kanwal, N., Hussain, S., Saleem, M., & Khan, I. A. (2021). Study of structural, optical and dielectric properties of ZnO/PVDF-based flexible sheets. Journal of Polymer Research, 28(8), 1–13. https://doi.org/10.1007/S10965-021-02640-9

[23] Buckley, D. H., McNulty, D., Zubialevich, V. Z., Parbrook, P. J., & O'Dwyer, C. (n.d.). Highly-Ordered Growth of Solution-Processable ZnO for Thin Film Transistors. https://doi.org/10.1149/ma2017-01/25/1219

[24] Zheng, H. J., Zhao, Z., Liu, Y. L., Zhao, X. F., & Xi, K. H. (2012). Preparation of PLA/Nano-ZnO Composites. Advanced Materials Research, 1901–1904. https://doi.org/10.4028/WWW.SCIENTIFIC.NET/AMR.476-478.1901

[25] Restrepo, I., Benito, N., Medinam, C., Mangalaraja, R. V., Flores, P., & Rodríguez-Llamazares, S. (2017). Development and characterization of polyvinyl alcohol stabilized polylactic acid/ZnO nanocomposites. 4(10), 105019. https://doi.org/10.1088/2053-1591/AA8B8D

[26] Rahimli, A., Huseynova, A., & Musayeva, N. (2024). Comprehensive analysis OF ZnO-Doped polystyrene nanocomposites: Structural, optical and defect analysis. Journal of Thermoplastic Composite Materials. https://doi.org/10.1177/08927057241291794

[27] Nonato, R. C., Innocnentini Mei, L. H., Bonse, B. C., Leal, C. V., Levy, C. E., Oliveira, F. A., Delarmelina, C., Duarte, M. C. T., & Morales, A. R. (2022). Nanocomposites of PLA / ZnO nanofibers for medical applications: Antimicrobial effect, thermal, and mechanical behavior under cyclic stress. Polymer Engineering and Science, **62**(4), 1147–1155. https://doi.org/10.1002/pen.25913

[28] Basavaraj, H. G., Renuka, C. G., Harihar, C. A., Sangappa, Y., Rao, B. L., & Madhukumar, R. (2020). Physicochemical mechanical and optical properties of polymer inorganic composite thin films: Applications. **2244**, 110009. https://doi.org/10.1063/5.0009947

[29] Klok, L. A., Steffen, T. T., Sabedra, H. R., Fontana, L. C., Hammer, P., Marega, F. M., Costa, L. C., Pessan, L. A., & Becker, D. (2023). ZnO surface modification with maleic anhydride using plasma treatment. Plasma Processes and Polymers. https://doi.org/10.1002/ppap.202300165

[30] Lauritsen, J. V., Porsgaard, S., Rasmussen, M. K., Jensen, M. C. R., Bechstein, R., Meinander, K., Clausen, B. S., Helveg, S., Wahl, R., Kresse, G., & Besenbacher, F. (2011). Stabilization Principles for Polar Surfaces of ZnO. ACS Nano, **5**(7), 5987–5994. https://doi.org/10.1021/NN2017606

ЕКСПЕРИМЕНТАЛЬНЕ ТА МОДЕЛЮВАЛЬНЕ ДОСЛІДЖЕННЯ СТРУКТУРНИХ, ОПТИЧНИХ ТА МЕХАНІЧНИХ ВЛАСТИВОСТЕЙ НАНОКОМПОЗИТІВ PLA/ZnO

Фахріддін Т. Юсупов[1], Тохірбек І. Рахмонов[1], Мехріддін Ф. Ахмаджонов[1], Ділобарбану Є. Абдукодірова[2], Єлмурат Досимов[3], Іфтихорджон Юльчієв[1]

[1]Ферганський державний технічний університет, Фергана, Узбекистан
[2]Чирчицький державний педагогічний університет, Чирчик, Узбекистан
[3]Міжнародний казахсько-турецький університет імені Ходжі Ахмеда Ясаві, Казахстан

У цій роботі представлено комплексне експериментальне та теоретичне дослідження нанокомпозитів на основі полілактиду (PLA), армованих наночастинками оксиду цинку (ZnO) з концентраціями 0,5, 1, 3 та 5 мас.%. Стан дисперсії та мікроструктурні особливості ZnO в матриці PLA досліджувалися за допомогою сканувальної електронної мікроскопії у поєднанні з енергодисперсійною рентгенівською спектроскопією, що виявило однорідний розподіл наповнювача за низького вмісту та поступове агломерування за вищих концентрацій. Аналіз рентгенівської дифракції підтвердив збереження гексагональної вюрцитної кристалічної структури ZnO після введення в полімерну матрицю, тоді як композиційно залежні зміни розміру кристалітів і мікродеформацій ґратки корелюють із механічною відповіддю композитів. Інфрачервона спектроскопія з перетворенням Фур'є свідчить про наявність міжфазних взаємодій між ланцюгами PLA та наночастинками ZnO, що проявляється у систематичних зсувах смуги валентних коливань карбонільної групи та пов'язаних із цим ефектах перерозподілу заряду. Ультрафіолетово-видима спектроскопія демонструє суттєве підвищення ефективності екранування ультрафіолетового випромінювання зі зростанням вмісту ZnO, що супроводжується появою підзонних смуг поглинання, зумовлених дефектними та міжфазними електронними станами. Розрахунки в межах теорії функціоналу густини підтверджують експериментальні результати, виявляючи міжфазний перенос заряду та незначні модифікації електронної структури на межі розділу PLA/ZnO. Отримані результати показують, що введення ZnO підвищує механічну жорсткість і ефективність УФ-захисту, при цьому оптимальний вміст ZnO нижче 1 мас.% забезпечує збереження механічної цілісності та мінімізує деградацію, спричинену агломерацією наночастинок.

Ключові слова: *нанокомпозити PLA/ZnO; УФ-захист; механічні властивості; рентгенівська дифракція (XRD); FTIR; DFT-моделювання; перенесення заряду; наноматеріали; полімерне армування*